ePublishing

ΕΘΝΙΚΟ ΚΕΝΤΡΟ ΤΕΚΜΗΡΙΩΣΗΣ
EKT
NATIONAL DOCUMENTATION CENTRE

HNPS Advances in Nuclear Physics

Vol 24 (2016)

HNPS2016

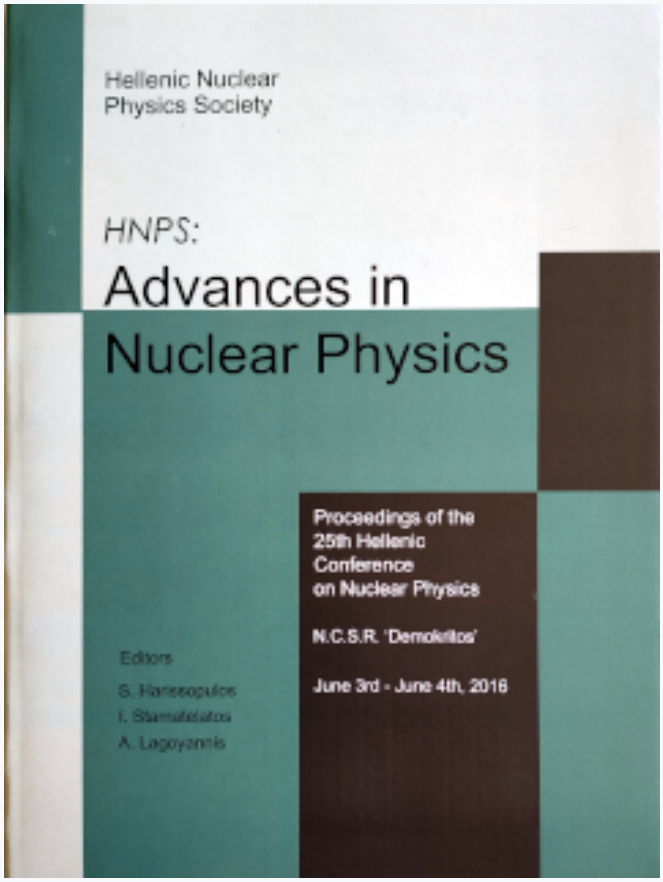

Neutron-induced fission cross-section measurement of 234U with monoenergetic beams in the keV and MeV range using MicroMegas detectors

A. Kanellakopoulos, A. Stamatopoulos, A. Tsinganis, M. Kokkoris, R. Vlastou, A. Kalamara, A. Lagoyannis, M. Axiotis

doi: 10.12681/hnps.1875

To cite this article:

Kanellakopoulos, A., Stamatopoulos, A., Tsinganis, A., Kokkoris, M., Vlastou, R., Kalamara, A., Lagoyannis, A., & Axiotis, M. (2019). Neutron-induced fission cross-section measurement of 234U with monoenergetic beams in the keV and MeV range using MicroMegas detectors. *HNPS Advances in Nuclear Physics*, *24*, 250–254. https://doi.org/10.12681/hnps.1875

https://epublishing.ekt.gr | **e-Publisher:** EKT | **Downloaded at:** 23/02/2026 20:15:18

Neutron-induced fission cross-section measurement of ^{234}U with monoenergetic beams in the keV and MeV range using MicroMegas detectors

A. Kanellakopoulos[1,*], A. Stamatopoulos[1], A. Tsinganis[1,2], M. Kokkoris[1], R. Vlastou[1], A. Kalamara[1], A. Lagoyannis[3], M. Axiotis[3]

[1] *Department of Physics, National Technical University of Athens, 157 80 Greece*
[2] *European Organisation for Nuclear Research (CERN), Geneva, Switzerland*
[3] *Institute of Nuclear and Particle Physics, National Centre for Scientific Research "Demokritos", Athens, 153 10 Greece*

Abstract The fission cross-section of ^{234}U was measured at incident neutron energies between 300 and 500 keV and 4 and 5 MeV with a setup based on "microbulk" MicroMegas detectors. The standard ^{235,238}U fission cross-sections were used as reference. The neutron beams were produced via the ^{7}Li(p,n) and the ^{2}H(d,n) reactions at the neutron beam facility of the 5.5 MeV Tandem accelerator laboratory at NCSR "Demokritos". The mass of the actinide content of the targets used and of their impurities was quantitatively determined via α – spectroscopy. The developed methodology and preliminary results are presented.

Keywords Fission, neutrons, cross section, micromegas, ^{234}U

INTRODUCTION

Accurate data on neutron-induced fission cross-sections of actinides are essential for the design of advanced nuclear reactors based on fast neutron spectra and alternative fuel cycles, as well as for the reduction of safety margins of existing and future conventional facilities. Meanwhile, there are significant discrepancies in the experimental cross section datasets available in literature. In the case of ^{234}U(n,f) the cross section data shown in fig. 1, present discrepancies of the order of 40% at some energies. In order to study these discrepancies, the 5.5 MeV Tandem accelerator at INPP lab of NSCR "Demokritos" was employed to carry out fission cross section measurements in the energy region 450-650 keV & 5.5-10 MeV implementing an assembly of MicroMegas detectors.

NEUTRON SOURCES

The ^{7}Li(p,n)^{7}Be reaction can provide monoenergetic neutrons with energies from threshold upto a few hundreds of keV, while for neutrons in the MeV rangethe ^{2}H(d,n)^{3}He reaction is widely employed.

Thin films of LiF evaporated on Tantalum substrates were used as targets for protons to produce the neutron beam in the 400-700 keV region via the ^{7}Li(p,n)^{7}Be reaction. Each target

* Corresponding author, email: tassoskan@yahoo.gr

was mounted in an externally air cooled flange to maintain the vacuum in the beam line and avoid the evaporation of the LiF target. This is a strictly monoenergetic forward-peaked reaction up to En= 550 keV, where a second family of neutrons appears via the first excited state of ^{7}Be.

The neutron beam in the MeV region was produced by the bombardment of a deuterium gas shell target with the use of the ^{2}H(d,n)^{3}He reaction. The 3.7cm gas shell is fitted with a 5μm Molybdenium thin entrance foil and a 1mm Platinum beam stop. The whole gas shell is air-cooled to ensure the structural integrity of the Molybdenium foil, while the pressure was around 1-1.3 bar and remotely controlled and monitored.

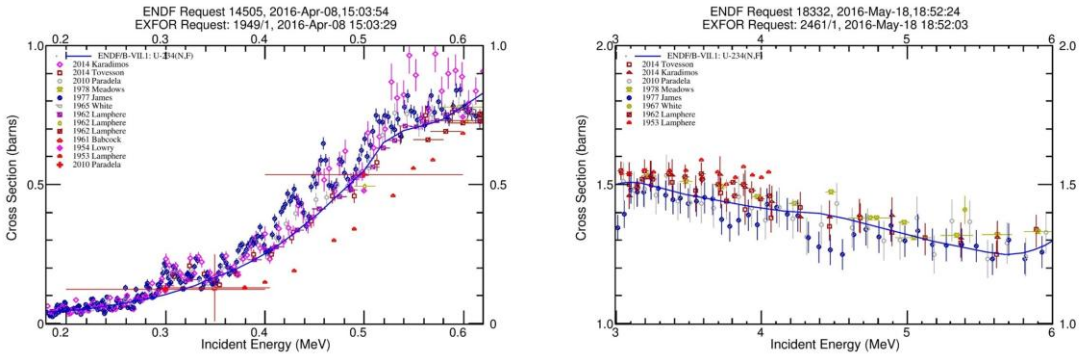

Fig. 1. ^{234}U(n,f) cross section with both ENDF online evaluation library and experimental data. On the left the low-energy cross section is presented, while on the rightthe high-energy one

THE MICROMEGAS DETECTOR

For the purpose of the experiment, a "microbulk" MicroMegas (Micro-MEsh GAseous Structure) detector system, manufactured at CERN for NTUA, has been employed. The gas area between the anode and the cathode of a MicroMegas detector is separated by a thin micromesh structure. The drift region, where the primary ionization occurs, is 8mm wide while the amplification gap is 50μm, where the charge multiplication takes place. This detector is ideal for neutron physics since it minimizes the amount of materials in the path of the neutron beam.

A stainless steel chamber with thin kapton windows at both ends capable of holding multiple targets and detectors was used as experimental chamber. The chamber was filled with a circulating Ar:CO_2 (85%-15%) gas mixture at atmospheric pressure.

A full optimization of the detector system was carried out to determine the optimal functionality conditions. The pad (cathode) was grounded and by changing the drift voltage (anode), while keeping the mesh voltage steady, the transparency curve for every detector was determined (see left part of fig. 2), where the ability of the charge of the primary ionization to drift to the amplification area is tested. To determine the gain curve, where the

charge multiplication in the amplification area is tested, voltage at drift was steady while mesh voltage was being changed.

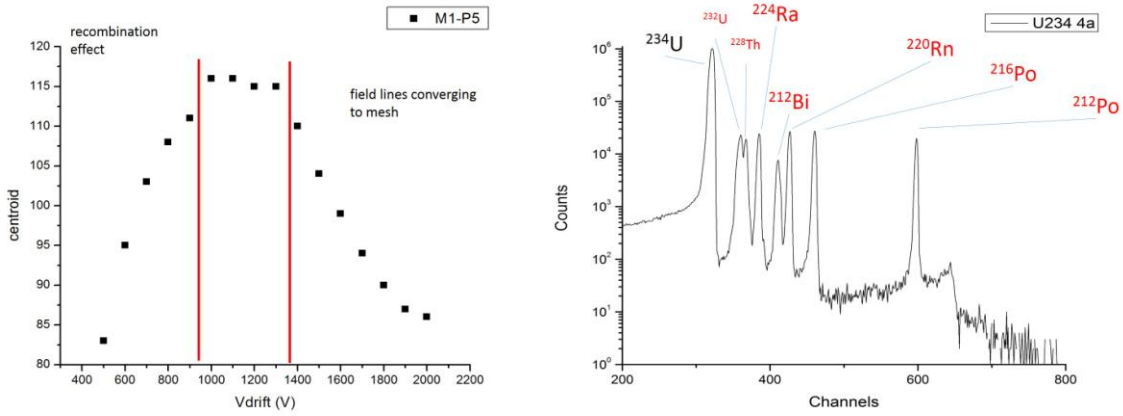

Fig. 2. Transparency curve of a MicroMegas detector (left). α-particle spectrum of ^{234}U, using a SSB detector. Impurities from the short-lived ^{232}U and its decay chain are present in the target with a mass estimation of ~ 10^{-5} gr (right).

TARGETS

The actinide targets were manufactured in IPPE, Obninsk and JINR, Dubna, using the painting technique and were originally used at n_TOF. Along with the targets of ^{234}U, targets of ^{235}U and ^{238}U were used as reference. All the targets come in the form of U_3O_8 and were covered with Aluminum masks with a hole of 4cm in diameter to reduce the α-activity of the Uranium targets, and to avoid errors in geometry or inhomogeneities that may appear at the edges of each target due to the adopted manufacturing technique.

The mass and the impurities of the targets were determined using α-spectroscopy. A typical spectrum is shown in the right part of Fig. 2. The Uranium targets are mainly α-emitters and the mass of the Uranium content is the ratio of the α-activity of the target in 4π *(C)* to the specific activity of the isotope *(C_s)* which is a characteristic constant of an isotope, depending on its half life ($t_{1/2}$) and mass number *(A)* (for long-lived isotopes. The activity in 4π cannot be measured directly. So, since the α-emission is isotropic, the activity *(C_Ω)* in a specific solid angle *(Ω)* is measured instead and then the activity in 4π is determined. Thus for the mass of a certain isotope in the target one gets:

A big SSB detector with an active surface of 30 cm^2 with a tantalum mask of 5.8 cm in diameter was used to determine the α-activity. The mask secured the minimization of edge effects and shadow effects from the inactive areas of the detector. The energy calibration was

accomplished using a ^{241}Am source and the solid angle of the disk-to-disk geometry was determined using the SACALC Monte-Carlo package.

EXPERIMENTAL RESULTS AND ANALYSIS

In order to study in detail the production and propagation through the experimental setup of the neutron beam, Monte-Carlo simulations were employed. In this direction the *NeuSDesc* (Neutron Source Description) code, developed at JRC-IRMM (Geel, Belgium), was used to obtain the energy spectrum, flux and angular distribution of the produced neutrons for each source reaction and incoming beam energy. The output of this code is then, used as a neutron source input for the MCNP code, where the full geometry of the rest of the experimental setup is described, scoring the neutron flux down to thermal energies at each target.

The experimental energy spectrum for ^{234}U is presented in fig. 4. Despite the multiple pile up of α-particles present in the spectrum, the separation of α-particles and fission fragments is evident. The fission fragment energy distribution is also clear.

For each incident neutron energy, the ^{234}U(n,f) total cross-section will be determined with respect to the ^{235}U(n,f) one. Detailed MCNP simulations have been carried out to take into account the geometry corrections of the neutron flux among the different targets in the MicroMegas assembly. The neutron flux was double checked using γ-spectroscopy and the 478 keV γ-ray of ^{7}Be from the activated LiF foils.

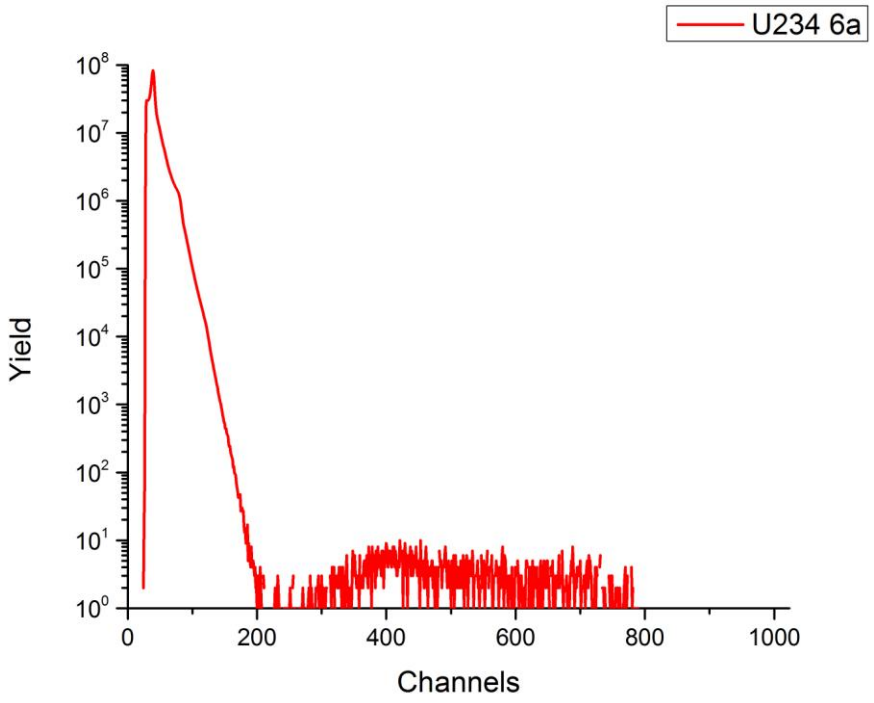

Fig. 4. Typical fission fragment spectrum of ^{234}U. The distribution of the light and the heavy fission fragment is apparent.

CONCLUSIONS

A full optimization of the detection system of the MicroMegas assembly was carried out, where all the properties of the gaseous detector were tested and the optimal settings of operation were determined. At the same time, a full evaluation of the Uranium targets was performed to test their mass and impurities content. A combination of Monte-Carlo codes was also used to study the production and propagation of the neutron beam from the neutron production target to the Micromegas assembly chamber, for both p+^{7}Li and d+^{2}H reactions. The analysis of the experimental fission spectra is currently in progress over the whole energy range studied in the present work. In addition, Monte-Carlo simulations to evaluate fission fragments self –absorption in the targets and the contribution of fission fragments under the α-peak are performed. After this detailed analysis process, the cross section of ^{234}U(n,f) will be determined with respect to the reference reaction ^{235}U(n,f).

References

[1] Evaluated Nuclear Data File (ENDF), www-nds.iaea.org/exfor/endf.htm
[2] Experimental Nuclear Reaction Data (EXFOR), www-nds.iaea.org/exfor/exfor.htm
[3] Average Solid Angle SACLC3, sites.google.com/site/averagesolidangle2/dow/sacalc3
[4] E. Birgersson, G. Lovestam, Tech. Rep. EUR 23794 EN, JRC-IRMM (2009)
[5] J. Ziegler, Stopping and Range of Ions in Matter, SRIM 2013, www.srim.org
[6] X-5 Monte Carlo team, "NCNP-A General Monte Carlo N-Particle Transport Code, version 5", Volume I-III, LA-UR-03-1987, LA-CP-03-0245 and LA-CP-03-0284, April (2003).